Emerging, hydrogen-driven electrochemical water purification

M.E. Suss [a,b,c,*], Y. Zhang [d,e], I. Atlas [f], Y. Gendel [g,*], E.B. Ruck [g], V. Presser [d,e,h,*]

[a] *Faculty of Mechanical Engineering, Technion – Israel Institute of Technology, Haifa, Israel*
[b] *Wolfson Department of Chemical Engineering, Technion – Israel Institute of Technology, Haifa, Israel*
[c] *Grand Technion Energy Program, Technion – Israel Institute of Technology, Haifa, Israel*
[d] *INM – Leibniz Institute for New Materials, Campus D22, 66123 Saarbrücken, Germany*
[e] *Department of Materials Science and Engineering, Saarland University, Campus D22, 66123 Saarbrücken, Germany*
[f] *Russell Berrie Nanotechnology Institute, Technion – Israel Institute of Technology, Haifa, Israel*
[g] *Faculty of Civil and Environmental Engineering, Technion – Israel Institute of Technology, Haifa, Israel*
[h] *Saarene, Saarland Center for Energy Materials and Sustainability, Campus D42, 66123 Saarbrücken, Germany*

ARTICLE INFO

ABSTRACT

Energy-efficient technologies for the remediation of water and generation of drinking water is a key towards sustainable technologies. Electrochemical desalination technologies are promising alternatives towards established methods, such as reverse osmosis or nanofiltration. In the last few years, hydrogen-driven electrochemical water purification has emerged. This review article explores the concept of desalination fuel cells and capacitive-Faradaic fuel cells for ion separation.

1. Introduction

1.1. State-of-the-art in water purification

While 71% of the earth is covered by water, freshwater occupies only 2.5% of the total water and is mostly stored as glaciers, ice caps, and groundwater [1]. With the rapid economic growth and urbanization, access to clean water for all human beings has become inadequate [2]. On average, 10% of the global population lives in countries with high or critical water stress [3]. Under this circumstance, an array of measures must be taken to mitigate clean water scarcity. One active method of securing clean water supplies is seawater and brackish water desalination. Conventional desalination technologies can be classified into thermal energy-driven, mechanical energy-driven, and electrical energy-driven [4].

As the earliest water desalination method, water evaporation and condensation are applied in thermal energy-driven technologies such as multi-stage flash distillation (MSF) and multi-effect distillation (MED) [5]. By using multiple steps, water from brines is evaporated and condensed to freshwater. Mechanical energy-driven desalination technologies, such as reverse osmosis (RO), are based on semipermeable membranes, which enable water molecules to be transported through

while rejecting salt ions. By applying pressure to the feedwater above its osmotic pressure, freshwater can be extracted from seawater [6]. Typically, the energy efficiency of RO is higher than the thermal-energy-driven technologies for seawater desalination [7]. As for electrical energy-driven desalination technologies, the major types include electrodialysis (ED) [8,9], a mature technology explored for the past six decades, and the emerging technology of capacitive deionization (CDI) [10] and desalination batteries [11,12]. The latter two immobilize salt ions into capacitive or Faradaic electrode materials [11]. Such systems are highly promising towards ion selective separations and brackish water desalination, but require a cyclic, two-stage charge-discharge process, during which energy is alternatingly stored and released by electrodes [13].

In recent years, a chemical-driven class of desalination technologies has emerged. Such cells are often distinct because of the form of the input energy and because they can co-generate electricity and clean water [14]. Hydrogen can be used as one of the necessary chemical reactants to drive such processes. Particularly attractive is green hydrogen, which leverages renewable energies such as solar, wind, and hydropower energies. Hydrogen gas is a well-known reducing agent in water treatment processes, for example, in dehalogenation of organic compounds [15], phenol reduction into less toxic cyclohexane [16],

catalytic hydrogenation to convert nitrite and nitrate into N_2 and ammonia [17,18], and catalytic reduction of ClO_4^- and BrO_3^- by H_2 gas into Cl^- and Br^-, respectively [19,20]. Hydrogen may also be used indirectly for ion separations. For example, Al-Hallaj et al. proposed a fuel cell desalination system that uses the electricity and exhaust heat from the fuel cells to power RO or MSF units [21].

While hydrogen has had a role in water treatment as a reducing agent or indirectly driving separations, it was only recently that hydrogen had been explored towards directly driving separations using a single electrochemical cell. Two types of such cells have emerged in the past three years, including desalination fuel cells (DFCs) and capacitive-Faradaic fuel cells (CFFCs; Fig. 1). This very recent technological advancement

has resulted in a fast-growing number of publications. We here will review and discuss the emerging field of direct hydrogen-driven electrochemical water purification.

1.2. Desalination fuel cells for simultaneous production of clean water and electricity

The DFC has its roots in ED, where a typical ED cell contains a pair of membranes, one anion exchange, and the other cation, and is driven by a voltage or current applied to a pair of electrodes sandwiching the cell [8,30]. Several classical ED cells and stacks have been explored in recent years, including shock ED [31], bipolar ED [32], and multi-stage ED
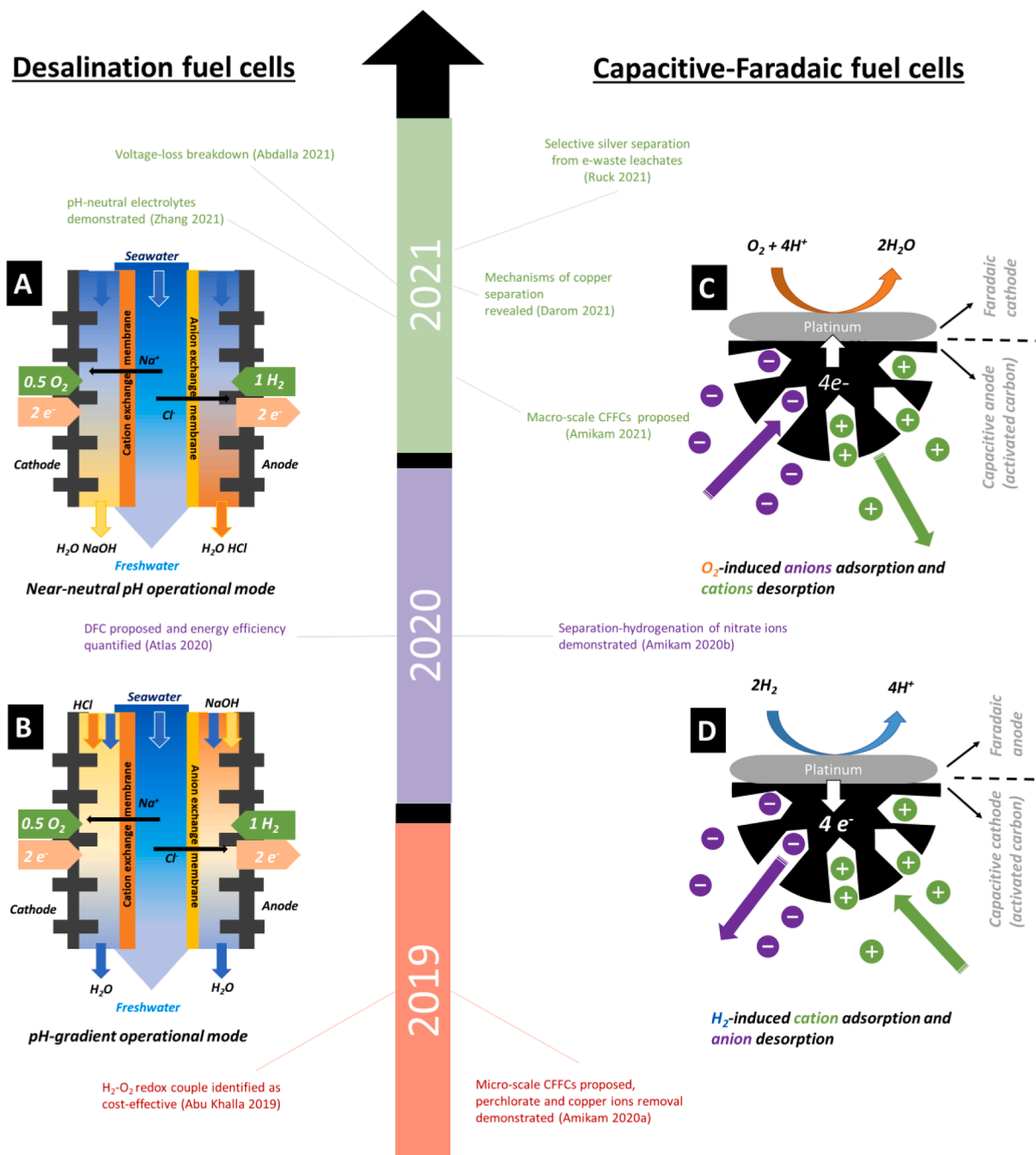
Fig. 1. Timeline on the development of hydrogen-driven water purification technologies, including the desalination fuel cell (DFC) [14,22–24] and capacitive-Faradaic fuel cells (CFFC) [25–29]. Also provided are schematics showing the operational modes of a-b) the DFC, and c-d) the CFFC. List of references: Abdalla 2021: [23]; Abu Khalla 2019: [24]; Amikam 2020a: [25]; Amikam 2020b: [28]; Amikam 2021: [26]; Atlas 2020: [14]; Darom 2021: [27]; Ruck 2021: [29]; Zhang 2021: [22].
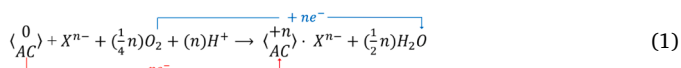
[33]. Another variation is the use of chemical energy rather than electrical energy to drive the separation [24,34]. This technique is unique because it allows the cell to drive separation and generate net electricity simultaneously [35]. In contrast to microbial desalination cells [36], these ED systems are driven by inorganic redox couples but do not employ microbes as microorganisms can limit electricity production and salt removal rates. ED cells driven by chemical energy perform a combined reaction-separation process that is thermodynamically spontaneous [14]. Atlas et al. calculated the maximum available energy from this combined process and quantified the thermodynamic efficiency of cells driven by chemical energy, finding that for specific chemistries, up to 25 kWh of net electricity per m^3 of treated seawater can be produced [14]. This technology can thus generate significant excess electricity, well above what is that needed for pre-treatment and post-treatment of the feed, which is approximately 1 kWh/m^3 [6].

One feature of chemical energy-driven ED is many possible redox couples which can be used to drive the process, each with potential benefits and drawbacks. Thus far, this concept has been tested with a small subset of possible chemistries, including zinc-bromine [24], zinc-air [37,38], aluminum-air [35], hydrogen-oxygen [14,22], and acid-base couples [39]. Among these, the hydrogen-oxygen couple is particularly promising, as it relies on relatively inexpensive gas-phase reactants, and the likely product of the chemical reaction is simply water. Cells that use the hydrogen-oxygen chemistry are termed "desalination fuel cells", depicted in Fig. 1A-B [14]. Other cell chemistries that rely on liquid-solvated reactants or that produce a waste product can complicate brine disposal. The use of hydrogen can also lead to an important and growing role for water treatment in the hydrogen economy. The main drawback of using the hydrogen-oxygen redox couple is the need to often-expensive metal-based catalysts for the oxygen reduction and hydrogen oxidation reactions.

1.3. Capacitive-Faradaic fuel cells for ion separation

The *electrolytic* water treatment reactors such as electrocoagulation, electrodialysis, and electrooxidation can be classified as Faradaic cells because they contain anodes and cathodes where oxidation and reduction (i.e., Faradaic processes) take place. The *galvanic* desalinating Faradaic cells are powered by oxidants (i.e., oxygen) and fuels (e.g., hydrogen) which are reacted on cathode and anode, respectively [22,34]. In *capacitive* cells, the electrical current is mostly non-Faradaic; that is, both the anode and cathode act as capacitors charged within an application of an external voltage source, which results in electrosorption of ions and capacitive deionization (CDI) of water [40,41]. The capacitive-Faradaic cells contain both the Faradaic and the capacitive electrodes; that is, during the operation, the oxidation or the reduction processes proceed on one electrode, and the electrosorption takes place on the counter electrode. Capacitive-Faradaic cells that separate ionic pollutants or valuable ions from water and wastewater can be electrolytic or galvanic [42,43]. Amikam et al. have recently proposed capacitive-Faradaic cells powered by hydrogen and oxygen gases [25].

Micro-scale capacitive-Faradaic fuel cells (CFFCs) comprise activated carbon (AC) particles loaded with nanoscale platinum catalyst crystals. Upon immersion of CFFCs into an aerated aqueous solution, the oxygen reduction reaction (ORR) on the platinum catalyst (the Faradaic electrode) consumes the electrons from the AC (the capacitive electrode) that results in adsorption of anions into the electrical double-layer of electron-deficient AC to maintain its electroneutrality, as described by Eq. (1) ($\langle {}^0_{AC} \rangle$ – uncharged activated carbon; $\langle {}^{+n}_{AC} \rangle \cdot X^{n-}$ – activated carbon that lost n electrons within the electrosorption of X^{n-} anion) [25].

$$\langle {}^0_{AC} \rangle + X^{n-} + (\tfrac{1}{4}n)O_2 + (n)H^+ \xrightarrow[- ne^-]{+ ne^-} \langle {}^{+n}_{AC} \rangle \cdot X^{n-} + (\tfrac{1}{2}n)H_2O \tag{1}$$

The electrosorption of anions proceeds until the complete saturation of the electrical double-layer in the CFFC. The saturated cells must be regenerated, and the anions released into the concentrate solution. The regeneration of the CFFCs is accomplished via the hydrogen oxidation reaction (HOR) on Pt that results in the accumulation of electrons in the activated carbon and a release of anions into a brine solution (Eq. (2)).

$$\langle {}^{+n}_{AC} \rangle \cdot X^{n-} + (\tfrac{1}{2}n)H_2 \xrightarrow[+ ne^-]{- ne^-} \langle {}^0_{AC} \rangle + X^{n-} + (n)H^+ \tag{2}$$
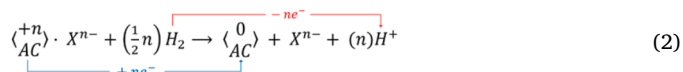
Overall, the anions in the treated solution are "replaced" with electrogenerated hydroxyl ions (OH$^-$). The principle of ions separation by capacitive-Faradaic cells is shown in Fig. 1C-D.

The separation of cations can be achieved if ORR follows HOR. In this case, the removed cations are compensated in solution by the anodically produced hydronium ions (H$_3$O$^+$) [25]. The undivided electrodes of the CFFCs establish different potentials in hydrogenated or aerated aqueous solutions, and this cell potential drives electrosorption, HOR, and ORR. Thus, at pH=7, the CFFC's open-cell potentials in aerated and hydrogenated NaCl solution approaches 200 mV and 760 mV, respectively [26]. The separation of ions by CFFCs is powered by the chemical energy of hydrogen and oxygen gases. However, the micro-scale CFFCs originally proposed by Amikam et al. [25] do not generate an electrical current that can be used for powering an external load. In this respect, the micro-scale CFFCs are different from the classical fuel cells and the macro-scale divided CFFCs which can produce electricity [26].

2. Thermodynamics underpinning desalination fuel cells

The DFC is distinct from other desalination technologies, as it does not perform solely a separation process, but a combined chemical reaction and separation process. To evaluate the thermodynamics energy efficiency (TEE) of a desalination fuel cell (DFC), we cannot use the same methods used for MSF, RO, ED, and CDI, where TEE is defined as the energy required in practice divided by the minimum energy of the reversible separation process. For a DFC, TEE is the ratio of experimentally extracted electricity per desalinated water volume, w_e, to maximum available energy per desalinated water volume, w, giving TEE $\equiv w_e/w$ [14]. The parameter w can be decomposed to $w = w_{chem} + w_S$, where w_{chem} and w_S are chemical and the separation work per desalinated water volume. We define w_{chem} as the change in Gibbs free energy per desalinated water volume of H$^+$ and OH$^-$ between the initial and complete reactant consumption states (Eq. (3)) [14]:

$$w_{chem} = \Delta c \left[F\left(E_c^0 - E_a^0\right) + 2RT ln\left(\frac{c_{B|A}}{c^0}\right) \right] \tag{3}$$

E_c^0 is the standard potential of the cathode half-reaction, E_a^0 of the anode half-reaction, F Faraday's constant, Δc is the change in concentration of the feedwater over the process, R the ideal gas constant, T the absolute temperature, and c^0 is the concentration at standard state, which is 1 M. Further, $c_{B|A}$ is the initial concentration of acid/base in the catholyte/anolyte, respectively. We invoke assumptions such as neglecting the crossover of reactants or products and assuming ideally selective membranes. Complete reactant consumption is attained at the maximal water recovery $\phi_{max} = \left(2\Delta c/c_{B|A} + 1\right)^{-1}$, here the complete utilization of H$^+$ and OH$^-$ in catholyte and anolyte, respectively.

Similarly, we define w_S as the change in Gibbs free energy per volume of desalinated water of both Na^+ and Cl^- between the initial and final states. For complete consumption of the reactants, we obtain w_s via Eq. (4):

$$w_S = 2RT \left[c_{NaCl}^F ln\left(\frac{c_{NaCl}^F}{c^0}\right) - (c_{NaCl}^F - \Delta c) ln\left(\frac{c_{NaCl}^F - \Delta c}{c^0}\right) \right]$$

$$+ \frac{2\Delta cRT}{c_{B|A}} \left[\begin{array}{l} (c_{NaCl}^F + c_{B|A}) ln\left(\frac{c_{NaCl}^F + c_{B|A}}{c^0}\right) \\ - (c_{NaCl}^F + 2c_{B|A}) ln\left(\frac{c_{NaCl}^F + 2c_{B|A}}{c^0}\right) \end{array} \right] \tag{4}$$

Here, c_{NaCl}^F is the initial salt concentration of the feedwater.

In Fig. 2, we show calculations of w, for a DFC, as a function of the acidity (basicity) of the catholyte (anolyte). As can be seen, more energy is available per m³ of treated water for increasing pH gradient between the anode and cathode (Fig. 1B), as expected since this increases the available neutralization energy. For example, for a cell operating with neutral pH anolyte and catholyte (Fig. 1A), the available energy remains below 20 kWh/m³. In contrast, for a cell with an anolyte of pH 0 and a catholyte of pH 14, the available energy is well over 30 kWh/m³. As shown by Abdalla et al., [23] the voltage losses in near-neutral pH operating mode are much more severe, especially at low currents, making it more difficult to extract near-to the maximum available energy level for that operating mode. The pH gradient mode, by contrast, limits voltage losses and allows for extracting electrical energy closer to the maximum available energy.

3. Electrode materials and performance

3.1. Desalination fuel cell performance

The DFC concept is in its infancy, with only a handful of experimental reports thus far. In 2019, Khalla et al. performed a preliminary techno-economic analysis of chemical-driven ED cells, finding that hydrogen-oxygen redox couple was highly promising due to its reliance on low-cost reactants [24]. In 2020, Atlas et al. built and characterized a DFC with a cell containing three flows, an anolyte pumped between the anode and anion exchange membrane, a catholyte between a cathode and cation exchange membrane, and a feedwater channel between the two membranes [14]. Their cell utilized an acidic catholyte and alkaline anolyte to boost open-circuit voltage (and so electricity production), termed pH gradient operational mode [14]. They found that the cell had an open circuit voltage of about 1.7 V, and desalinated a 0.5 M NaCl stream at a current efficiency of circa 80% [14]. The electrical production was quantified via TEE, where TEE of the DFC reached up to 68% at
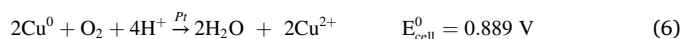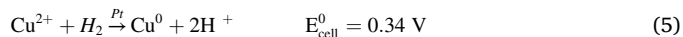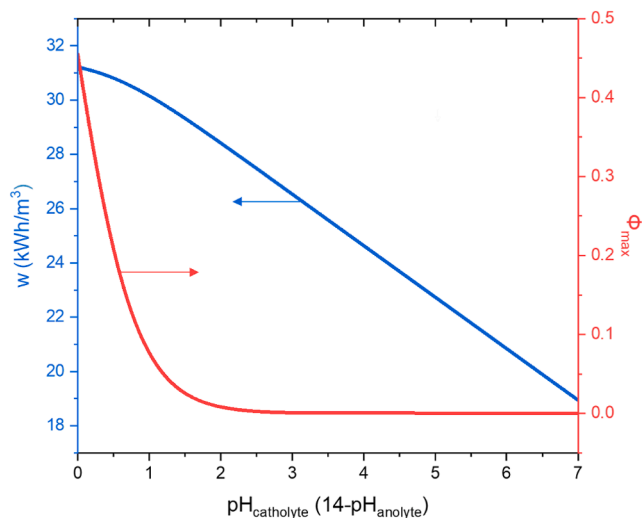

Fig. 2. Calculated maximum available energy from a desalination fuel cell, w, versus the pH of the anolyte and catholyte streams. Also plotted is the maximum water recovery, ϕ_{max}.

low current densities of about 1 mA/cm², and efficiency dropped as extracted current density was increased [14]. This efficiency was lower than that achieved for other chemistries, such as zinc-bromine chemistry. In 2021, Zhang et al. demonstrated a DFC which operated without acid and base in the anolyte and catholyte, respectively, which is termed the "near-neutral pH" operational mode [22]. They reported relatively low cell voltages of < 0.7 V, which limited electricity production to 67 mWh per 1 g NaCl removed while desalinating a 0.6 M NaCl feed [22].

Possible reasons for the low energy efficiencies and energy production of the cells of Atlas et al. [14] and Zhang et al. [22] was determined by Abdalla et al., [23] who performed a voltage loss breakdown in a DFC operating both in near-neutral and pH gradient operational modes. They incorporated quasi-reference Ag/AgCl electrodes into each of the three channels of a DFC prototype, allowing independent measurement of electrode voltages and voltage drops across membranes [23]. Major Nernstian losses occurred at the cathode in both operational models [23]. The reason proposed for these losses was the poisoning of the platinum cathode catalyst by chloride ions, which shifted the oxygen reduction reaction to the less-energetic two-electron pathway, which produces hydrogen peroxide. As shown in a recent work by Abu Khalla et al., when adjusting the TEE calculation to account for solely two-electron oxygen reduction, and operating in pH gradient mode, TEE was reported to be up to 95.6% [44]. Significant activation losses were seen in the near-neutral pH operational mode, both at the anode and cathode, which at the cathode was determined to be largely due to low H^+ concentration rather than Pt poisoning [44]. The latter work served to highlight the importance of catholyte composition and cathode catalyst material in DFC performance, and provides several pathways for improvement for future DFC designs.

3.2. Capacitive-Faradaic fuel cell performance

First, the H_2-powered capacitive-Faradaic separation of ions was proven for ClO_4^- removal [25]. Aeration of 480 mL NaClO₄ solution $([ClO_4^-]_0 = 212$ mg/L) on 12 g of 5 mass%-loaded Pt CFFCs (further termed 5.0%Pt-CFFCs) resulted in circa 80% of ClO_4^- ions removal. The salt adsorption capacity (SAC) of the microscale CFFCs was 0.06 meq/g (equivalent to 3.5 mg$_{NaCl}$/g), which is significantly lower than the SAC values reported for regular CDI (3.7–13.0 mg$_{NaCl}$/g) [25]. Fig. 3A shows the results of ClO_4^- ions removal from pure NaClO₄ solutions using the CFFC that comprised 5.0% and 0.1% of Pt catalyst on a granular activated carbon. As it appears in Fig. 3A, a 50-fold decrease in the platinum loading did not result in any significant performance decrease of the CFFCs for ClO_4^- removal. This finding shows that effective CFFCs with a low Pt load and a competitive cost can be developed for environmental applications.

In the original study of Amikam et al., [25]. The separation of copper by the CFFCs was demonstrated, and Cu^{2+} ions separation was initially attributed to the capacitive-Faradaic mechanism explained above [25]. Darom et al. showed that separation of copper ions by the Pt-loaded carbon is governed not by the electrosorption but rather by the Pt-catalyzed reduction of Cu^{2+} (Eq. (5)) and oxidation of elemental Cu particles into Cu^{2+} (Eq. (6)) in H_2-induced and O_2-induced steps of the process, respectively [27]. Fig. 3B shows the Cu crystals formed within the hydrogenation of pure CuCl₂ solution on the CFFCs.

$$Cu^{2+} + H_2 \xrightarrow{Pt} Cu^0 + 2H^+ \qquad E_{cell}^0 = 0.34 \text{ V} \tag{5}$$

$$2Cu^0 + O_2 + 4H^+ \xrightarrow{Pt} 2H_2O + 2Cu^{2+} \qquad E_{cell}^0 = 0.889 \text{ V} \tag{6}$$

Recently Ruck et al. [29] reported on the selective recovery of silver ions using the Pt-catalyzed hydrogenation-oxygenation process proposed by Darom at al. [27].

The CFFCs were also shown effective for the separation of nitrate ions [28]. Moreover, the CFFCs with bimetallic 5%Pt-1%Cu catalyst resulted in a complete reduction of nitrate ions into the N_2 (selectivity of
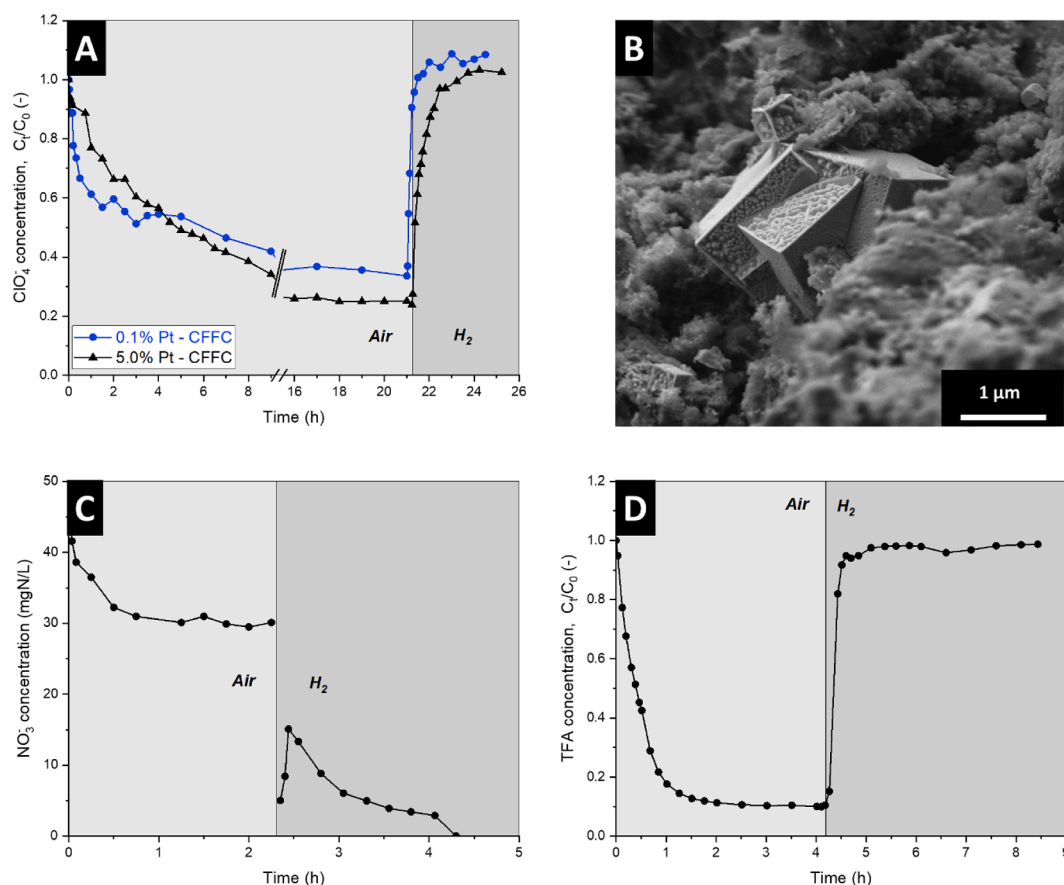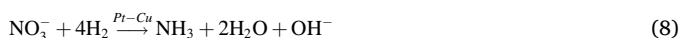
Fig. 3. Results of oxygenation-hydrogenation of perchlorate, copper, nitrate and trifluoracetic acid (TFA) solutions in a batch mode system operated with 7.5 g of CFFCs of granular activated carbon (CH104, mesh size 12–20, Spectrum) [28]. (A) Separation of perchlorate ions ($[ClO_4^-]_0 = 200$ mg/L, 300 mL); (B) Scanning electron micrograph of the crystals of elemental Cu formed on the 0.1%Pt-CFFC within the hydrogenation of $CuCl_2$ solution ($[Cu^{2+}]_0 = 500$ mg/L, pH = 0, 1 L); (C) Separation-hydrogenation of nitrates in $NaNO_3$ solution ($[NO_3^-]_0 = 300$ mg/L, 300 mL) using 1.0%Pt-0.2%In-CFFCs. After the air-induced separation the $NaNO_3$ solution was replaced with 300 mL of deionized water for the hydrogenation step. (D) Separation of TFA using 0.5%Pt-CFFCs ($[TFA]_0 = 5$ mg/L, 1 L).

ca. 55%) gas and ammonia within the hydrogenation step of the process (Eq. (7) and (8)) [28]:

$$2NO_3^- + 5H_2 \xrightarrow{Pt-Cu} N_2 + 4H_2O + 2OH^- \qquad (7)$$

$$NO_3^- + 4H_2 \xrightarrow{Pt-Cu} NH_3 + 2H_2O + OH^- \qquad (8)$$

Besides Pt-Cu other catalysts can be applied for nitrite and nitrate hydrogenation by the CFFCs [45]. Fig. 3C shows the results of nitrate separation and hydrogenation conducted using the 1.0%Pt-0.2%In-CFFCs that comprised 1.0% platinum and 0.2 % indium (In) metals in granular activated charcoal. The selectivity of the process towards the N_2 gas was as high as about 90%.

CFFCs have many other potential applications for removal of hazardous anionic compounds, for instance, the highly toxic trifluoroacetic acid exists in water mostly as a trifluoroacetate anion that can be separated by electrosorption and by the CFFCs. Fig. 3D shows the results of the oxygenation-hydrogenation cycle of TFA solution in a batch mode system with 0.5%Pt-CFFCs.

Experiments aimed at separating Na^+ and NH_4^+ by the micro-scale or undivided macro-scale CFFCs revealed that electrosorption of these cations is very poor [26]. This phenomenon was attributed to an influence of H^+ cations (produced within the HOR) that occupy the activated carbon surface or/and create the low local pH in the CFFCs, resulting in the positively charged surface of the CFFCs and repulsion of cations [26].

The main potential advantage of the micro-scale CFFCs is that no wiring, spacers, or gaskets are required for the process that can be performed in simple packed-bed or fluidized-bed reactors. The second advantage is that regeneration of the (electro)adsorbent does not involve the application of acids, salts, or bases. Cons include utilization of expensive Pt catalyst, low salt adsorption capacity, and co-production of H^+ and OH^- ions that occupy SAC of the CFFCs and even prevent separation of cations. Further studies are required to reveal the mechanisms of ions separation, develop mechanistic models describing the kinetics, decrease Pt-loading or use of non-noble metal catalysts, increase selectivity towards the specific pollutants, and to develop a process with an efficient H_2 gas utilization.

4. Outlook, and next steps

With its almost 100-year history, fuel-cells have not stopped bringing forth novel technologies [46]. There is no indication that hydrogen-driven technologies will tire in the future of being an engine to innovation and provide opportunities towards sustainability. Hydrogen as the fuel for water remediation requires careful consideration of the eco-balance. Today, 95% of the hydrogen production relates to non-renewable sources, such as coal and gas [47]. The global efforts towards a more sustainable, industrialized world will require transformative changes and monumental investments so that renewable energy combined with electrolysis and other green hydrogen generation pathways will make an impact. Yet, even today, already 5% of the global hydrogen production relates to hydrogen being a by-product of other chemical processes, foremost chlorine production [47]. Thereby, the future adaptation of hydrogen-driven water purification may also

extend to other by-product gases, such as methane.

As for the material- and system-related challenges, it will be essential to establish both robust long-term performance metrics and to strive towards the use of lower-cost electrode materials. Finding a good balance between high performance, stability, use of abundant materials, use of low-cost materials, and competition with other desalination technologies will be a critical challenge.

CRediT authorship contribution statement

M.E. Suss: Conceptualization, Writing – original draft, Writing – review & editing, Visualization. **Y. Zhang:** Writing – review & editing, Visualization. **I. Atlas:** Writing – review & editing, Visualization. **Y. Gendel:** Conceptualization, Writing – original draft, Writing – review & editing, Visualization. **E.B. Ruck:** Writing – review & editing, Visualization. **V. Presser:** Conceptualization, Writing – original draft, Writing – review & editing, Visualization.

Declaration of Competing Interest

The authors declare that they have no known competing financial interests or personal relationships that could have appeared to influence the work reported in this paper.

References

[1] A. Alkaisi, R. Mossad, A. Sharifian-Barforoush, A Review of the Water Desalination Systems Integrated with Renewable Energy, Energy Proc. 110 (2017) 268–274.

[2] A.Y. Hoekstra, M.M. Mekonnen, A.K. Chapagain, R.E. Mathews, B.D. Richter, Global Monthly Water Scarcity: Blue Water Footprints versus Blue Water Availability, PLoS ONE 7 (2012), e32688.

[3] Progress on the level of water stress. Global status and acceleration needs for SDG indicator 6.4.2, FAO and UN Water, 2021.

[4] R. Epsztein, R.M. DuChanois, C.L. Ritt, A. Noy, M. Elimelech, Towards single-species selectivity of membranes with subnanometre pores, Nat. Nanotechnol. 15 (2020) 426–436.

[5] D. Curto, V. Franzitta, A. Guercio, A Review of the Water Desalination Technologies, Appl. Sci. 11 (2021) 670.

[6] M. Elimelech, W.A. Phillip, The Future of Seawater Desalination: Energy, Technology, and the Environment, Science 333 (2011) 712–717.

[7] K.C. Ng, M. Burhan, Q. Chen, D. Ybyraiymkul, F.H. Akhtar, M. Kumja, R.W. Field, M.W. Shahzad, A thermodynamic platform for evaluating the energy efficiency of combined power generation and desalination plants, NPJ Clean Water 4 (2021) 25.

[8] H. Strathmann, Electrodialysis, a mature technology with a multitude of new applications, Desalination 264 (2010) 268–288.

[9] S. Al-Amshawee, M.Y.B.M. Yunus, A.A.M. Azoddein, D.G. Hassell, I.H. Dakhil, H. A. Hasan, Electrodialysis desalination for water and wastewater: A review, Chem. Eng. J. 380 (2020), 122231.

[10] M.E. Suss, S. Porada, X. Sun, P.M. Biesheuvel, J. Yoon, V. Presser, Water desalination via capacitive deionization: what is it and what can we expect from it? Energy Environ. Sci. 8 (2015) 2296–2319.

[11] P. Srimuk, X. Su, J. Yoon, D. Aurbach, V. Presser, Charge-transfer materials for electrochemical water desalination, ion separation and the recovery of elements, Nat. Rev. Mater. 5 (7) (2020) 517–538.

[12] M.E. Suss, V. Presser, Water Desalination with Energy Storage Electrode Materials, Joule 2 (1) (2018) 10–15.

[13] M. Metzger, M.M. Besli, S. Kuppan, S. Hellstrom, S. Kim, E. Sebti, C.V. Subban, J. Christensen, Techno-economic analysis of capacitive and intercalative water deionization, Energy Environ. Sci. 13 (6) (2020) 1544–1560.

[14] I. Atlas, S. Abu Khalla, M.E. Suss, Thermodynamic Energy Efficiency of Electrochemical Systems Performing Simultaneous Water Desalination and Electricity Generation, J. Electrochem. Soc. 167 (13) (2020) 134517, https://doi.org/10.1149/1945-7111/abb709.

[15] B.T. Meshesha, N. Barrabés, J. Llorca, A. Dafinov, F. Medina, K. Föttinger, PdCu alloy nanoparticles on alumina as selective catalysts for trichloroethylene hydrodechlorination to ethylene, Appl. Catal. A 453 (2013) 130–141.

[16] E. Díaz, A.F. Mohedano, L. Calvo, M.A. Gilarranz, J.A. Casas, J.J. Rodríguez, Hydrogenation of phenol in aqueous phase with palladium on activated carbon catalysts, Chem. Eng. J. 131 (2007) 65–71.

[17] F. Ruiz-Beviá, M.J. Fernández-Torres, Effective catalytic removal of nitrates from drinking water: An unresolved problem? J. Clean. Prod. 217 (2019) 398–408.

[18] P. Xu, S. Agarwal, L. Lefferts, Mechanism of nitrite hydrogenation over Pd/γ-Al$_2$O$_3$ according a rigorous kinetic study, J. Catal. 383 (2020) 124–134.

[19] K.D. Hurley, J.R. Shapley, Efficient Heterogeneous Catalytic Reduction of Perchlorate in Water, Environ. Sci. Technol. 41 (2007) 2044–2049.

[20] H. Chen, Z. Xu, H. Wan, J. Zheng, D. Yin, S. Zheng, Aqueous bromate reduction by catalytic hydrogenation over Pd/Al$_2$O$_3$ catalysts, Appl. Catal. B 96 (2010) 307–313.

[21] S. Al-Hallaj, F. Alasfour, S. Parekh, S. Amiruddin, J.R. Selman, H. Ghezel-Ayagh, Conceptual design of a novel hybrid fuel cell/desalination system, Desalination 164 (2004) 19–31.

[22] Y. Zhang, L. Wang, V. Presser, Electrocatalytic fuel cell desalination for continuous energy and freshwater generation, Cell Rep. Phys. Sci. 2 (2021), 100416.

[23] S. Abdalla, S.A. Khalla, M.E. Suss, Voltage loss breakdown in desalination fuel cells, Electrochem. Commun. 132 (2021), 107136.

[24] S. Abu Khalla, M.E. Suss, Desalination via chemical energy: An electrodialysis cell driven by spontaneous electrode reactions, Desalination 467 (2019) 257–262.

[25] G. Amikam, N. Manor-Korin, P. Nativ, Y. Gendel, Separation of ions from water and wastewater using micro-scale capacitive-faradaic fuel cells (CFFCs), powered by H$_2$(g) and air, Sep. Purif. Technol. 253 (2020), 117494.

[26] G. Amikam, Y. Gendel, Capacitive-faradaic fuel cells (CFFCs) for ion separation: Macro-scale configurations and polarization mechanism, Electrochem. Commun. 124 (2021), 106945.

[27] Y. Darom, G. Amikam, E.B. Ruck, Y. Gendel, Capacitive-faradaic fuel cells (CFFCs) for selective separation of copper(II) ions from water and wastewater, Chem. Eng. J. 421 (2021), 129950.

[28] G. Amikam, Y. Gendel, Separation and hydrogenation of nitrate ions by micro-scale capacitive-faradaic fuel cells (CFFCs), Electrochem. Commun. 120 (2020), 106831.

[29] E.B. Ruck, G. Amikam, Y. Darom, N. Manor-Korin, Y. Gendel, Catalytic selective recovery of silver from dilute aqueous solutions and e-waste leachates, Sep. Purif. Technol. (2021) 120303, https://doi.org/10.1016/j.seppur.2021.120303.

[30] M. Tedesco, H.V.M. Hamelers, P.M. Biesheuvel, Nernst-Planck transport theory for (reverse) electrodialysis: I. Effect of co-ion transport through the membranes, J. Membrane Sci. 510 (2016) 370–381.

[31] S. Schlumpberger, N.B. Lu, M.E. Suss, M.Z. Bazant, Scalable and Continuous Water Deionization by Shock Electrodialysis, Environ. Sci. Technol. Lett. 2 (12) (2015) 367–372.

[32] H. Lu, L.i. Wang, R. Wycisk, P.N. Pintauro, S. Lin, Quantifying the kinetics-energetics performance tradeoff in bipolar membrane electrodialysis, J. Membrane Sci. 612 (2020) 118279, https://doi.org/10.1016/j.memsci.2020.118279.

[33] G.J. Doornbusch, M. Bel, M. Tedesco, J.W. Post, Z. Borneman, K. Nijmeijer, Effect of membrane area and membrane properties in multistage electrodialysis for seawater desalination performance, J. Membrane Sci. 611 (2020) 118303, https://doi.org/10.1016/j.memsci.2020.118303.

[34] I. Atlas, M.E. Suss, Theory of simultaneous desalination and electricity generation via an electrodialysis cell driven by spontaneous redox reactions, Electrochim. Acta 319 (2019) 813–821.

[35] S.M. Shariatpannahi, M.S. Hatamipour, S. Rashid-Nadimi, M.K. Amini, Simultaneous saltwater desalination and power generation using an aluminum-powered cell, J. Environ. Chem. Eng. 9 (2) (2021) 104802, https://doi.org/10.1016/j.jece:2020.104802.

[36] Y. Kim, B.E. Logan, Microbial desalination cells for energy production and desalination, Desalination 308 (2013) 122–130.

[37] J. Dai, N.L. Win Pyae, F. Chen, M. Liang, S. Wang, K. Ramalingam, S. Zhai, C.-Y. Su, Y. Shi, C. Tan, L. Zhang, Y. Chen, Zinc-Air Battery-Based Desalination Device, ACS Appl. Mater. Interfaces 12 (23) (2020) 25728–25735.

[38] P. Srimuk, L. Wang, Ö. Budak, V. Presser, High-performance ion removal via zinc-air desalination, Electrochem. Commun. 115 (2020) 106713, https://doi.org/10.1016/j.elecom.2020.106713.

[39] Z.M. Bhat, D. Pandit, S. Ardo, R. Thimmappa, A.R. Kottaichamy, N. Christudas Dargily, M.C. Devendrachari, M. Ottakam Thotiyl, An Electrochemical Neutralization Cell for Spontaneous Water Desalination, Joule 4 (8) (2020) 1730–1742.

[40] S. Porada, R. Zhao, A. van der Wal, V. Presser, P.M. Biesheuvel, Review on the science and technology of water desalination by capacitive deionization, Prog. Mater. Sci. 58 (8) (2013) 1388–1442.

[41] Y.M. Volfkovich, Capacitive Deionization of Water (A Review), Russ. J. Electrochem. 56 (2020) 18–51.

[42] J. Chang, F. Duan, H. Cao, K. Tang, C. Su, Y. Li, Superiority of a novel flow-electrode capacitive deionization (FCDI) based on a battery material at high applied voltage, Desalination 468 (2019), 114080.

[43] Y. Xu, F. Duan, Y. Li, H. Cao, J. Chang, H. Pang, J. Chen, Enhanced desalination performance in asymmetric flow electrode capacitive deionization with nickel hexacyanoferrate and activated carbon electrodes, Desalination 514 (2021), 115172.

[44] S. Abu Khalla, I. Atlas, S. Litster, M.E. Suss, Desalination Fuel Cells with High Thermodynamic Energy Efficiency, Environ. Sci. Technol. (2022), https://doi.org/10.1021/acs.est.1c07288.

[45] J. Martínez, A. Ortiz, I. Ortiz, State-of-the-art and perspectives of the catalytic and electrocatalytic reduction of aqueous nitrates, Appl. Catal. B 207 (2017) 42–59.

[46] W. Vielstich, Handbook of Fuel Cells, 2010.

[47] Green hydrogen: A guide to policy making, International Renewable Energy Agency, 2020.